

1 **Title: Cortical selectivity driven by connectivity: Innate connectivity patterns of**  
2 **the visual word form area**

3

4 Authors: Jin Li, David E. Osher, Heather A. Hansen, Zeynep M. Saygin

5 **Affiliation:** Department of Psychology & Center for Cognitive and Brain Sciences, The  
6 Ohio State University

7

8 Please address correspondence to:

9 Jin Li, Department of Psychology, The Ohio State University, 225 Psychology Building,  
10 1835 Neil Avenue, Columbus, OH, 43210. E-mail: [li.9361@osu.edu](mailto:li.9361@osu.edu)

11 and

12 Zeynep M. Saygin, Department of Psychology, The Ohio State University, 225  
13 Psychology Building, 1835 Neil Avenue, Columbus, OH, 43210. E-mail:  
14 [saygin.3@osu.edu](mailto:saygin.3@osu.edu)

15

16

17

18

19

## Abstract

20 The human brain is a patchwork of different functionally specialized areas. What  
21 determines this functional organization of cortex? One hypothesis is that innate  
22 connectivity patterns shape functional organization by setting up a scaffold upon which  
23 functional specialization can later take place. We tested this hypothesis here by asking  
24 whether the visual word form area (VWFA), an experience-driven region that only  
25 becomes selective to visual words after gaining literacy, was already connected to proto  
26 language networks in neonates scanned within one week of birth. We found that  
27 neonates showed adult-like functional connectivity, and observed that i) the VWFA  
28 connected more strongly with frontal and temporal language regions than regions  
29 adjacent to these language regions (e.g., frontal attentional demand, temporal auditory  
30 regions), and ii) language regions connected more strongly with the putative VWFA than  
31 other adjacent ventral visual regions that also show foveal bias (e.g. fusiform face area,  
32 FFA). Object regions showed similar connectivity with language areas as the VWFA but  
33 not with face areas in neonates, arguing against prior hypotheses that the region that  
34 becomes the VWFA starts out with a selectivity for faces. These data suggest that the  
35 location of the VWFA is earmarked at birth due to its connectivity with the language  
36 network, providing novel evidence that innate connectivity instructs the later refinement  
37 of cortex.

## 38 INTRODUCTION

39 Decades of research suggest that the adult brain is composed of patches of cortex that  
40 are specialized for unique mental functions. To what extent is the functional  
41 organization of the human brain innate? Recent advances in developmental  
42 neuroimaging have made it possible to start to answer this question. For example, a  
43 recent study showed category-selective responses in high-level visual cortex for faces  
44 and scenes in infants<sup>1</sup>. Moreover, research in congenitally blind individuals suggests  
45 that cortical selectivity for high-level visual categories may not require visual  
46 experience<sup>2</sup>. In addition to the early emergence of visual processing, a previous study  
47 also found a neural precursor of language processing in infants<sup>3</sup>. Specifically, they  
48 found brain activity in left superior temporal and angular gyri to human speech in 3-  
49 month-old infants. These studies support the protomap hypothesis, which suggests that  
50 early genetic instructions give rise to the mature functional areas of the cortex.  
51 However, the driving factor of this early functional specialization remains ambiguous.

52 The Connectivity Hypothesis proposes that the specialization of a given brain region  
53 is largely shaped by how it connects and communicates with the rest of the brain.  
54 Alternative (but not mutually exclusive) hypotheses are that the location of a given brain  
55 region is determined by its intrinsic molecular or circuit properties or, in the case of  
56 visual areas, by pre-existing featural or retinotopic biases that predispose a region to  
57 become selective to foveal or peripheral stimuli (Retinotopic Hypothesis)<sup>4-7</sup>. Previous  
58 work showed that structural connectivity (via diffusion imaging) can predict the  
59 functional selectivity of a brain region to different visual categories (i.e., faces, scenes,  
60 objects, bodies)<sup>8, 9</sup>. Functional connectivity (FC) (through resting-state scans) can also

61 be used to predict selectivity to various functional selectivity across the brain<sup>10-12</sup>. This  
62 work suggests that, at least in adults, connectivity is tightly intertwined with functional  
63 selectivity.

64 Few studies have examined whether early connectivity patterns may earmark cortical  
65 tissue as the future site of a functionally specific region. A resting-state FC study in  
66 macaques found that while newborn macaques deprived of faces did not show face-  
67 selective responses, they did show a proto-organization for retinotopy throughout the  
68 visual system<sup>13</sup>. This study supports the Connectivity Hypothesis as well as the  
69 Retinotopic Hypothesis, by suggesting that connectivity with early visual areas may set  
70 up a retinotopic scaffold upon which early viewing behavior, paired with the right type of  
71 input (e.g. faces) may then bias domain formation in stereotyped locations in high-level  
72 visual cortex. However, there likewise exists highly experience-dependent visual  
73 regions that are also in stereotyped locations, like the visual word form area (VWFA),  
74 which responds strongly to visual words or letter strings and only exists in literate  
75 individuals<sup>14, 15</sup>. How does the VWFA differentiate from the adjacent fusiform face area  
76 (FFA)? The perception of both words and faces requires the analysis of high-spatial  
77 frequency and foveal input<sup>16-18</sup>, and thus connectivity to early retinotopic areas may not  
78 differentiate them. Alternatively, the VWFA may become increasingly selective to visual  
79 words and may be differentiated from FFA by communicating with other regions, e.g.  
80 the language network. Thus, contrasting the development of the VWFA vs. FFA will help  
81 disentangle the Connectivity Hypothesis from the Retinotopic Hypothesis.

82 In adults, the VWFA connects with perisylvian language cortex, differentiating it  
83 from adjacent visual cortex<sup>19</sup>; other studies also found that white matter fibers that

84 originated from the VWFA pass through fascicles that may be critical for language  
85 processing<sup>20, 21</sup>. In children, a longitudinal study found that connectivity patterns in pre-  
86 literate 5-year-olds predicted the location of the VWFA in each child at age 8 after they  
87 learned to read, and differentiated it from the adjacent FFA<sup>22</sup>. The connectivity patterns  
88 that predicted the VWFA included putative language areas, suggesting that connectivity  
89 to these regions may earmark the future location of a visual region that is selective to  
90 words, and also set up a scaffold upon which future functional specialization can take  
91 place. However, while the 5-year-olds could not read (and at that age, lacked neural  
92 selectivity to letters or letter-like stimuli), they still would have had years of visual  
93 experience with letters and words. Is the putative VWFA already connected differently  
94 and set up to be differentiated from adjacent visual regions, even at birth? Alternatively,  
95 is the VWFA recycled from the adjacent FFA<sup>7</sup> or other adjacent regions; in other words,  
96 is the VWFA undifferentiated from the FFA in terms of its connectivity to language areas  
97 in neonates?

98 Here, we tested this proto-organization of the VWFA in the newborn brain. Based on  
99 the Connectivity Hypothesis, we hypothesized that although the VWFA is highly  
100 experience-dependent, it is already 'prewired' to be selective for visual words by  
101 communicating with proto language regions at birth. Specifically, by examining  
102 neonates who were scanned within one week of birth, we asked i) Does the VWFA  
103 show adult-like FC with the temporal and inferior frontal language network compared  
104 with adjacent regions like the multiple-demand (MD) network, speech regions, and  
105 primary auditory cortex (A1)? ii) Are connections stronger between language areas and

106 the cortical tissue of the putative VWFA, than with other visual areas within the ventral  
107 temporal cortex?

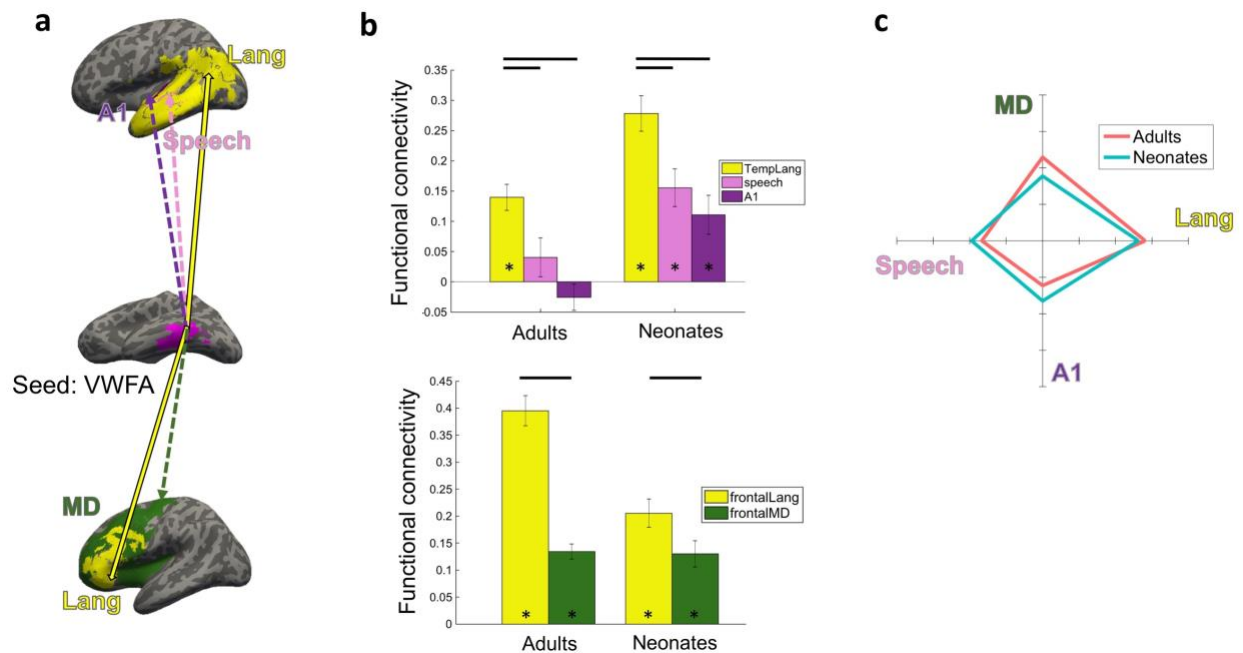
108

109

## 110 **RESULTS**

### 111 **FC between the putative VWFA and language regions**

112 We examined whether the putative VWFA already showed adult-like FC patterns even  
113 at birth. First, we asked, does this cortical tissue connect more to language regions vs.  
114 regions in the vicinity of language areas? We identified the putative VWFA, frontal and  
115 temporal language regions; as a comparison, we also included frontal multiple-demand  
116 (MD) regions (which activate during a wide variety of cognitively demanding tasks),  
117 speech regions in perisylvian cortex that don't respond preferentially to language but  
118 rather more generally to human speech sounds (much like a higher order auditory  
119 cortex), and primary auditory cortex (A1) (see Online Methods; **Fig. 1a**). The regions  
120 were defined in independent groups of adults and overlaid on the individual anatomical  
121 space of neonates and adults in this dataset (see Online Methods).



122

123 **Figure 1** FC between VWFA (seed) and non-visual regions (targets). **(a)** Functional  
 124 parcels overlaid on an example inflated brain and a schema of the connectivity analysis:  
 125 VWFA (magenta), language (yellow), speech (pink), A1 (purple), MD (dark green). **(b)**  
 126 Top, mean FC between VWFA and regions in temporal cortex. Bottom, mean FC  
 127 between VWFA and frontal language regions and MD regions. Connectivity values were  
 128 Fisher z transformed. Error bars denote s.e.m. Horizontal bars reflect significant *post*  
 129 *hoc* paired *t*-tests  $p < 0.05$ , corrected. **(c)**: FC fingerprint of VWFA. Connectivity values  
 130 were mean-centered and averaged within each of the four categories to plot the relative  
 131 patterns for the adult and neonate groups. TempLang, temporal language regions;  
 132 frontalLang, frontal language regions; frontalMD, frontal multiple-demand regions. \*  
 133 denotes significant one-sample *t*-test ( $p < 0.05$ ).

134

135 We calculated the functional connectivity (FC) between the VWFA (seed region) and  
 136 the language, MD, speech, and A1 regions (target regions). First, we examined the  
 137 VWFA's connectivity to temporal regions. We ran a 2-way ANOVA of age group  
 138 (neonate, adult)  $\times$  target (temporal language regions, speech, A1) and found significant  
 139 main effects for both target and age group (target:  $F(2,225) = 17.23$ ,  $p < 0.001$ ; age  
 140 group:  $F(1,225) = 30.51$ ,  $p < 0.001$ ), and no interaction between age group and target.

141 Both adults and neonates showed higher connectivity between the VWFA and language  
142 parcels compared with the connectivity between the VWFA and the adjacent speech  
143 region (**Fig. 1b**, top; *post-hoc t*-tests: adult:  $t(74) = 2.54$ ,  $p < 0.05$ , corrected, 95%  
144 confidence interval (CI) = [0.02, 0.18]; neonate:  $t(76) = 2.83$ ,  $p < 0.05$ , corrected; 95%  
145 CI = [0.04, 0.21]) and A1 (adult:  $t(74) = 5.29$ ,  $p < 0.001$ , corrected, 95% CI = [0.10,  
146 0.23]; neonate:  $t(76) = 3.79$ ,  $p < 0.001$ , corrected, 95% CI = [0.08, 0.26]).

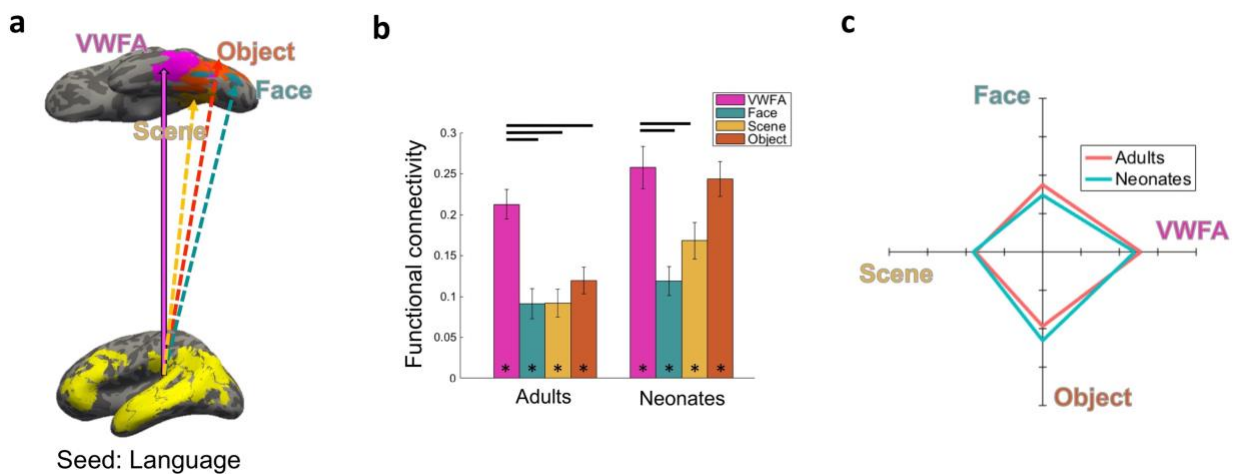
147 Next, since language regions also exist in frontal cortex, we explored the  
148 connectivity of the VWFA to frontal language regions. To control for potential distance or  
149 location confounds, we compared the connectivity between the VWFA to frontal  
150 language regions vs. the connectivity between the VWFA to frontal multiple-demand  
151 (MD) regions, which are intertwined with language regions but are functionally distinct  
152 from them (**Fig. 1a**). We first ran a 2-way ANOVA of age group (neonate, adult)  $\times$  target  
153 (frontal language, frontal MD) and found significant main effects for both target and age  
154 group (target:  $F(1,150) = 48.72$ ,  $p < 0.001$ ; age group:  $F(1,150) = 16.29$ ,  $p < 0.001$ ), and  
155 the interaction between target and age group was also significant ( $F(1,150) = 14.85$ ,  $p <$   
156  $0.001$ ). We found that the connectivity between the VWFA to frontal language regions  
157 was significantly higher than its connectivity to frontal MD regions (adult:  $t(74) = 8.23$ ,  $p$   
158  $< 0.001$ , corrected, 95% CI = [0.20, 0.32]; neonate:  $t(76) = 2.08$ ,  $p < 0.05$ , corrected,  
159 95% CI = [0, 0.15]) (**Fig. 1b**, bottom). These findings are summarized by the  
160 connectivity fingerprint plot in **Fig. 1c**, which indicates similar shapes (i.e., similar  
161 connectivity patterns) between neonates and adults. These results indicate that the  
162 cortical tissue that will later develop sensitivity to visual words have connectivity  
163 patterns that are relatively adult-like in the neonatal brain, suggesting that it is



164 earmarked to become functionally specialized by showing preferential connectivity with  
 165 language regions at birth.

166 **The selectivity of VWFA-language connections compared with other visual areas**

167 Next, we asked: do language regions selectively connect to the expected site of the  
 168 VWFA, compared with other adjacent high-level visual regions? To answer this  
 169 question, we compared the connectivity of language regions to the VWFA vs.  
 170 connectivity of language regions to other high-level visual areas in the ventral stream,  
 171 specifically in regions in the vicinity of the VWFA, including face selective regions  
 172 (Fusiform Face Area, FFA; Occipital Face Area, OFA), scene selective region  
 173 (Parahippocampal Place Area; PPA), and object selective regions (Lateral Occipital,  
 174 LO; Posterior Fusiform Sulcus, PFS) (**Fig. 2a**). These regions were overlaid on the  
 175 individual anatomical space as above (see Online Methods).

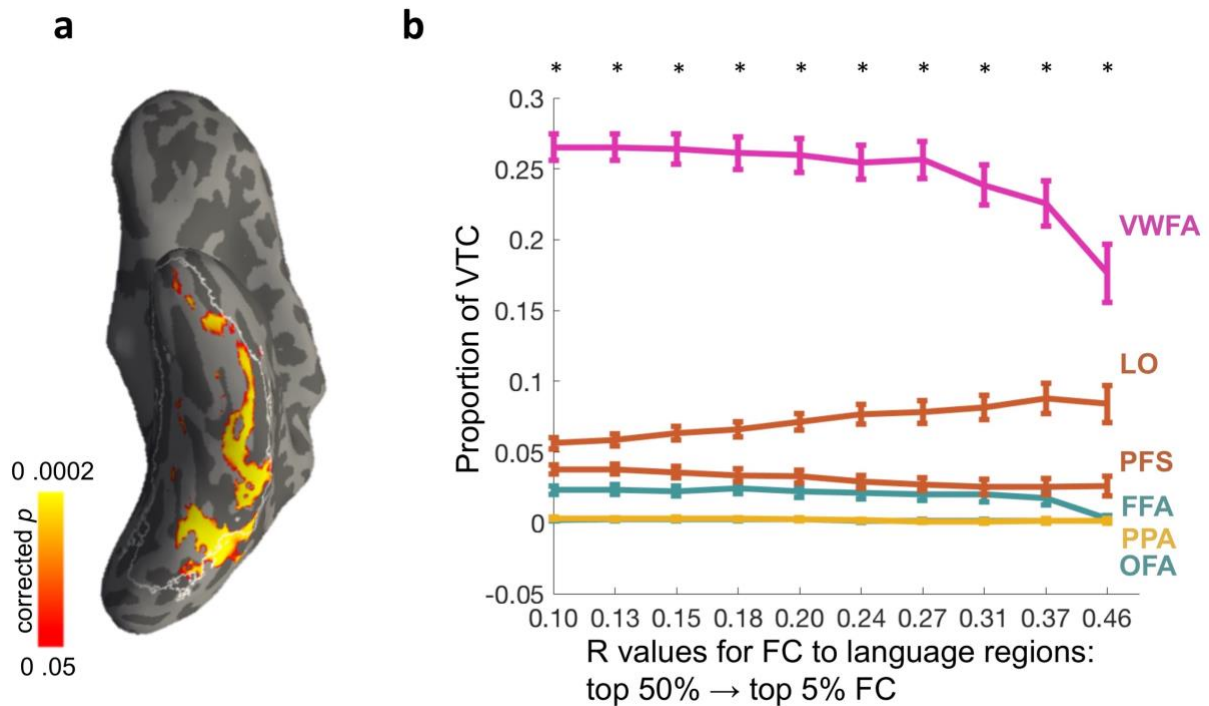


176

177 **Figure 2** FC between language regions (seed) and high-level visual regions (targets).  
 178 **(a)** Functional parcels and a schema of the connectivity analysis: language (yellow),  
 179 VWFA (magenta), faces (blue), scenes (gold), objects (orange) **(b)** Mean FC between  
 180 language regions and high-level visual regions in ventral visual stream. Connectivity

181 values were Fisher z transformed. Error bars denote s.e.m. Horizontal bars reflect  
182 significant *post hoc* paired *t*-tests  $p < 0.05$ , corrected. (c): FC fingerprint of language  
183 regions. Connectivity values were mean-centered and averaged within each of the four  
184 categories to plot the relative patterns for the adult and neonate groups. \* denotes  
185 significant one-sample *t*-test ( $p < 0.05$ ).

186 We ran a 2-way ANOVA of age group (neonate, adult)  $\times$  target (VWFA, faces,  
187 scenes, objects) and found significant main effects for both target and age group  
188 (target,  $F(3,300) = 16.32$ ,  $p < 0.001$ ; age group,  $F(1,300) = 22.88$ ,  $p < 0.001$ ; marginal  
189 significant interaction between target and age group ( $F(3,300) = 2.19$ ,  $p = 0.089$ ). *Post-*  
190 *hoc t*-tests revealed that in adults, the connectivity between language regions and the  
191 VWFA was significantly higher than all other high-level visual regions tested (face:  $t(74)$   
192  $= 4.64$ ,  $p < 0.001$ , corrected, 95% CI = [0.07, 0.17]; scene:  $t(74) = 4.80$ ,  $p < 0.001$ ,  
193 corrected, 95% CI = [0.07, 0.17]; object:  $t(74) = 3.80$ ,  $p < 0.001$ , corrected, 95% CI =  
194 [0.04, 0.14]) (**Fig. 2b**). The neonates showed a similar pattern, where connectivity  
195 between language regions and the VWFA was significantly higher than connectivity of  
196 language regions to face ( $t(76) = 4.39$ ,  $p < 0.001$ , corrected; scene, 95% CI = [0.08,  
197 0.20]:  $t(76) = 2.58$ ,  $p < 0.05$ , corrected, 95% CI = [0.02, 0.16]), but no difference  
198 between language regions' connectivity to the VWFA vs. object regions in neonates  
199 (**Fig. 2b**). These results indicate that neonates show an overall similar FC pattern as  
200 adults (**Fig. 2c**), with highest connectivity between language regions and VWFA;  
201 however, given that neonates show similar connectivity between language-VWFA and  
202 language-object regions, it suggests that there is further developmental refinement as  
203 functional specialization takes place.



204

205 **Figure 3** Voxel-wise analysis using language regions as the seed and each voxel within  
206 the ventral temporal cortex (VTC) as a target in the neonatal group. **(a)** Heatmap of  
207 voxels within VTC that are significantly connected with language regions (FWE-  
208 corrected by nonparametric permutation tests) and overlaid on an example brain. The  
209 white line denotes the VTC search space. **(b)** The proportion of VTC voxels that  
210 connect with language regions at increasing FC strengths, from the median to the top  
211 95<sup>th</sup> percentile, are plotted for each VTC region. Error bars denote s.e.m across  
212 participants. \* denotes significant paired *t*-test (VWFA vs. averaged of other functional  
213 regions,  $p < 0.05$ , corrected).

214

215 Next, to get a finer characterization of the connectivity between language regions  
216 and the whole ventral temporal cortex (VTC) in neonates, we performed a voxel-wise  
217 analysis within the VTC to explore which voxels connect most with language regions.  
218 One-sample *t*-tests were performed across neonates to identify voxels that are  
219 significantly connectivity with language regions (FWE corrected by nonparametric  
220 permutation tests,  $p < 0.05$ )<sup>23</sup>; these voxels were located mostly in the lateral fusiform

221 gyrus and a more posterior part of VTC (**Fig. 3a**). To identify which functional regions  
222 these voxels belonged to, we parametrically increased a threshold from the median to  
223 the top 95<sup>th</sup> percentile of FC across the VTC, and calculated the number of voxels within  
224 the VTC that were connected to language regions; we then quantified how many of  
225 these voxels belonged in each functional region (as a proportion of all VTC voxels that  
226 passed the threshold; Online Methods). We found that voxels that were connected to  
227 language regions were always located in the expected site of VWFA, above and beyond  
228 all other functional regions in the vicinity; this result was significant for all thresholds  
229 (**Fig. 3b**). We additionally did the same voxel-wise analysis in adult group, and again  
230 found that highest proportion of VTC voxels were located in VWFA compared with other  
231 adjacent high-level visual regions, which were significant for all threshold from the  
232 median to the top 95<sup>th</sup> percentile of FC.

233

## 234 **Discussion**

235 A mosaic-like functional organization is consistently found in the adult brain. However,  
236 the driving factor of this functional organization and its variation across individuals  
237 remains unclear. The Connectivity Hypothesis proposes that the future function of a  
238 given brain area is largely shaped by how this region connects with the rest of the brain.  
239 Other alternative accounts (that are not mutually exclusive with the Connectivity  
240 Hypothesis) are that other factors, such as retinotopic biases (i.e. Retinotopic  
241 Hypothesis) or other intrinsic cellular specialization, may set up a protomap for  
242 functional organization. Classic studies of 'rewired' ferrets showed that the cortical

243 region that would have developed into A1 took on many of the properties of V1 after  
244 retinal input was rerouted to that location, showing in animal models that connectivity  
245 precedes function<sup>24-28</sup>. Our findings extend this work from primary sensory cortex to  
246 high-level cortical regions in human neonates. In the present study, we investigated the  
247 connectivity patterns of the putative VWFA, a highly experience-dependent region, in  
248 the neonatal brain, and asked: is this region already pre-wired at birth to develop  
249 differential functional specialization from its neighbors? We found that the putative  
250 VWFA already shows adult-like connectivity patterns in neonates. Specifically, this  
251 cortical tissue may be earmarked to become selective to visual words by showing  
252 preferential connectivity with language regions. Moreover, the present study indicates  
253 that despite the early development of high-level visual cortex<sup>1</sup>, language regions  
254 specifically connect with the future site of VWFA compared with adjacent face and  
255 scene regions, just like adults. This research provides the earliest possible evidence in  
256 humans that the cortical tissue that will later develop sensitivity to visual words has a  
257 connectivity pattern at birth that makes it fertile-ground for such development – even  
258 before any exposure to words.

259 A recent study found that the VWFA has preferential FC with the core language  
260 system in adults<sup>29</sup>. Our study replicates this FC pattern, but importantly, we find that the  
261 preferential FC (and structural connectivity) between VWFA and language regions  
262 already exists in the neonatal brain. This result suggests that although neonates might  
263 not have a VWFA, this cortical tissue is already set up for its future function by showing  
264 higher connectivity with putative language regions. This provides strong evidence for  
265 the Connectivity Hypothesis of the functional organization of our brain. Moreover, our

266 results indicate that there is little, if any, communication between the VWFA and either  
267 A1 or the adjacent speech region, which is sensitive to the features of human speech  
268 (i.e., segmental and suprasegmental phonological properties). Infants within the first  
269 month of life show neural activation for speech vs. backwards speech<sup>3</sup>. Our results  
270 suggest that VWFA does not show preferential functional or structural connectivity with  
271 speech-selective regions in adults, but rather with adjacent language regions that are  
272 selective to higher-level semantic properties; further we show that this organization is  
273 present even at birth. These results suggest that the connectivity patterns of the  
274 putative VWFA are spatially precise even in newborns, and that phonemic  
275 representations for visual words may be accessed through other networks.

276 The VWFA serves as a good model to study the emergence of functionally selective  
277 regions. This region is highly experience-dependent and so it is almost certainly  
278 selective or shows preferential visual responses to another stimulus type (e.g., recycled  
279 from another high-level region) before the experience is gained. Previous studies  
280 posited that this cortical tissue starts out as part of the face network, and becomes  
281 increasingly selective to words and less selective to faces in the left hemisphere as  
282 literacy is acquired<sup>15, 30</sup>. This hypothesis is an attractive one because the perception of  
283 both faces and words require high-spatial frequency information that is represented  
284 foveally. Thus, with a retinotopic bias/connectivity from lower-level visual regions, it may  
285 be possible to first differentiate face regions from scene regions (foveal vs. peripheral  
286 bias) early in development (if not at birth), and then face from word regions after literacy  
287 is gained, perhaps through differential connections with fronto-temporal language  
288 regions. In contrast, our study finds evidence that the VWFA is in fact similar in its

289 connectivity with language regions as object regions, suggesting that the putative  
290 VWFA may first be undifferentiated from object regions. This result aligns with another  
291 study which found that young children's letter-recognition abilities may be related to  
292 their object recognition skills<sup>31</sup>. Moreover, a recent study shows that although the VWFA  
293 can be defined with words vs. faces in both skilled and struggling readers, the VWFA in  
294 struggling readers shows similar selectivity to words as it does to objects<sup>32</sup>. One  
295 possibility is that while the VWFA is already differentiated from face and scene areas at  
296 birth, it gains its selectivity to orthography through relevant experience and splits off  
297 from object cortex through repeated co-activations and further strengthening of its  
298 connections with language cortex. This hypothesis should be tested longitudinally to  
299 see how connections are strengthened and/or weakened as an individual gains literacy  
300 and as this piece of cortex begins to show preferential responses to orthography.

301 Another question that is raised by the present study is how the connectivity patterns  
302 themselves arose prenatally and evolutionarily. It is likely that a complex mechanism of  
303 intrinsic cellular or properties in different cortical regions and early signaling  
304 mechanisms set up these large-scale connections. It is possible that the VWFA is  
305 simply in a privileged location, due to a myriad of mechanisms including appropriate  
306 connections, cellular properties, and intrinsic circuitry, that facilitates its later selectivity.  
307 Future studies combining animal models with studies in other human populations, e.g.  
308 premature human infants, may help further elucidate these mechanisms.

309 A challenge of studying the functional organization of the neonatal brain is that there  
310 is no adequate way to localize functional responses using MRI in neonates. Here we

311 used functional regions from established studies and registered these regions to both  
312 adult and neonate brains using specialized software packages for infant image  
313 registrations. We also chose adjacent functional regions to test the spatial specificity of  
314 our findings. Future studies may consider new approaches to localize functional  
315 responses in young infants to further test the specificity of the current findings. Finally,  
316 we tested the Connectivity Hypothesis for the VWFA specifically. The findings suggest  
317 that connectivity-based scaffolding may be a general driving mechanism for the  
318 functional organization of human cortex, but the generality of this hypothesis for other  
319 mental domains remains to be tested.

320

## 321 **References**

- 322 1. Deen, B., *et al.* Organization of high-level visual cortex in human infants. *Nat Commun.*  
323 **8**, 13995 (2017).
- 324 2. van den Hurk, J., Van Baelen, M. & de Beeck, H.P.O. Development of visual category  
325 selectivity in ventral visual cortex does not require visual experience. *Proc Natl Acad Sci USA.*  
326 **114**, E4501-E4510 (2017).
- 327 3. Dehaene-Lambertz, G., Dehaene, S. & Hertz-Pannier, L. Functional neuroimaging of  
328 speech perception in infants. *Science.* **298**, 2013-2015 (2002).
- 329 4. Srihasam, K., Vincent, J.L. & Livingstone, M.S. Novel domain formation reveals proto-  
330 architecture in inferotemporal cortex. *Nat. Neurosci.* **17**, 1776 (2014).
- 331 5. Grill-Spector, K., Kourtzi, Z. & Kanwisher, N. The lateral occipital complex and its role  
332 in object recognition. *Vision research.* **41**, 1409-1422 (2001).



- 333 6. Dehaene, S. & Cohen, L. The unique role of the visual word form area in reading. *Trends*  
334 *Cogn Sci.* **15**, 254-262 (2011).
- 335 7. Dehaene, S. & Cohen, L. Cultural recycling of cortical maps. *Neuron.* **56**, 384-398  
336 (2007).
- 337 8. Osher, D.E., *et al.* Structural connectivity fingerprints predict cortical selectivity for  
338 multiple visual categories across cortex. *Cereb. Cortex.* **26**, 1668-1683 (2015).
- 339 9. Saygin, Z.M., *et al.* Anatomical connectivity patterns predict face selectivity in the  
340 fusiform gyrus. *Nat. Neurosci.* **15**, 321 (2012).
- 341 10. Osher, D.E., Brissenden, J.A. & Somers, D.C. Predicting an individual's Dorsal Attention  
342 Network activity from functional connectivity fingerprints. *J. Neurophysiol.* (2019).
- 343 11. Tobyne, S.M., *et al.* Prediction of individualized task activation in sensory modality-  
344 selective frontal cortex with 'connectome fingerprinting'. *Neuroimage.* **183**, 173-185 (2018).
- 345 12. Tavor, I., *et al.* Task-free MRI predicts individual differences in brain activity during task  
346 performance. *Science.* **352**, 216-220 (2016).
- 347 13. Arcaro, M.J. & Livingstone, M.S. A hierarchical, retinotopic proto-organization of the  
348 primate visual system at birth. *Elife.* **6**, e26196 (2017).
- 349 14. Baker, C.I., *et al.* Visual word processing and experiential origins of functional  
350 selectivity in human extrastriate cortex. *Proc Natl Acad Sci U S A.* **104**, 9087-9092 (2007).
- 351 15. Dehaene, S., *et al.* How learning to read changes the cortical networks for vision and  
352 language. *Science.* **330**, 1359-1364 (2010).
- 353 16. Malach, R., Levy, I. & Hasson, U. The topography of high-order human object areas. **6**,  
354 176-184 (2002).

- 355 17. Hasson, U., Levy, I., Behrmann, M., Hendler, T. & Malach, R. Eccentricity bias as an  
356 organizing principle for human high-order object areas. *Neuron*. **34**, 479-490 (2002).
- 357 18. Gomez, J., Barnett, M. & Grill-Spector, K. Extensive childhood experience with  
358 Pokémon suggests eccentricity drives organization of visual cortex. *Hum Nat*. **1** (2019).
- 359 19. Bouhali, F., *et al.* Anatomical connections of the visual word form area. *J Neurosci*. **34**,  
360 15402-15414 (2014).
- 361 20. Yeatman, J.D., Rauschecker, A.M. & Wandell, B.A. Anatomy of the visual word form  
362 area: adjacent cortical circuits and long-range white matter connections. *Brain Lang*. **125**, 146-  
363 155 (2013).
- 364 21. Epelbaum, S., *et al.* Pure alexia as a disconnection syndrome: new diffusion imaging  
365 evidence for an old concept. *Cortex*. **44**, 962-974 (2008).
- 366 22. Saygin, Z.M., *et al.* Connectivity precedes function in the development of the visual word  
367 form area. **19**, 1250 (2016).
- 368 23. Winkler, A.M., Ridgway, G.R., Webster, M.A., Smith, S.M. & Nichols, T.E.J.N.  
369 Permutation inference for the general linear model. **92**, 381-397 (2014).
- 370 24. Sur, M., Garraghty, P.E. & Roe, A.W. Experimentally induced visual projections into  
371 auditory thalamus and cortex. *Science*. **242**, 1437-1441 (1988).
- 372 25. Roe, A.W., Pallas, S.L., Hahm, J.-O. & Sur, M. A map of visual space induced in  
373 primary auditory cortex. *Science*. **250**, 818-820 (1990).
- 374 26. Roe, A.W., Pallas, S.L., Kwon, Y.H. & Sur, M. Visual projections routed to the auditory  
375 pathway in ferrets: receptive fields of visual neurons in primary auditory cortex. *J Neurosci*. **12**,  
376 3651-3664 (1992).

- 377 27. Sharma, J., Angelucci, A. & Sur, M. Induction of visual orientation modules in auditory  
378 cortex. *Nature*. **404**, 841 (2000).
- 379 28. Horng, S., *et al.* Differential gene expression in the developing lateral geniculate nucleus  
380 and medial geniculate nucleus reveals novel roles for Zic4 and Foxp2 in visual and auditory  
381 pathway development. *J Neurosci*. **29**, 13672-13683 (2009).
- 382 29. Stevens, W.D., Kravitz, D.J., Peng, C.S., Tessler, M.H. & Martin, A. Privileged  
383 functional connectivity between the visual word form area and the language system. *J Neurosci*.  
384 **37**, 5288-5297 (2017).
- 385 30. Dundas, E.M., Plaut, D.C. & Behrmann, M. The joint development of hemispheric  
386 lateralization for words and faces. *J Exp Psychol Gen*. **142**, 348-358 (2013).
- 387 31. Augustine, E., Jones, S.S., Smith, L.B. & Longfield, E. Relations among early object  
388 recognition skills: objects and letters. *Journal of Cognition and Development*. **16**, 221-235  
389 (2015).
- 390 32. Kubota, E.C., Joo, S.J., Huber, E. & Yeatman, J.D. Word selectivity in high-level visual  
391 cortex and reading skill. *Dev Cogn Neurosci*. (2018).
- 392 33. Makropoulos, A., *et al.* The developing human connectome project: A minimal  
393 processing pipeline for neonatal cortical surface reconstruction. *Neuroimage*. **173**, 88-112  
394 (2018).
- 395 34. Van Essen, D.C., *et al.* The WU-Minn human connectome project: an overview.  
396 *Neuroimage*. **80**, 62-79 (2013).
- 397 35. Hughes, E.J., *et al.* A dedicated neonatal brain imaging system. *Magn Reson Med*. **78**,  
398 794-804 (2017).

- 399 36. Makropoulos, A., *et al.* Automatic whole brain MRI segmentation of the developing  
400 neonatal brain. **33**, 1818-1831 (2014).
- 401 37. Zollei, L., Ou, Y., Iglesias, J., Grant, P. & Fischl, B. FreeSurfer image processing  
402 pipeline for infant clinical MRI images. *Hum Brain Mapp.* (2017).
- 403 38. de Macedo Rodrigues, K., *et al.* A FreeSurfer-compliant consistent manual segmentation  
404 of infant brains spanning the 0-2 year age range. *Front Hum Neurosci.* **9**, 21 (2015).
- 405 39. Fitzgibbon, S.P., *et al.* The developing Human Connectome Project (dHCP): minimal  
406 functional pre-processing pipeline for neonates. in *Fifth Biennial Conference on Resting State*  
407 *and Brain Connectivity* (2016).
- 408 40. Salimi-Khorshidi, G., *et al.* Automatic denoising of functional MRI data: combining  
409 independent component analysis and hierarchical fusion of classifiers. *Neuroimage.* **90**, 449-468  
410 (2014).
- 411 41. Behzadi, Y., Restom, K., Liau, J. & Liu, T.T.J.N. A component based noise correction  
412 method (CompCor) for BOLD and perfusion based fMRI. **37**, 90-101 (2007).
- 413 42. Glasser, M.F., *et al.* The minimal preprocessing pipelines for the Human Connectome  
414 Project. *Neuroimage.* **80**, 105-124 (2013).
- 415 43. Fedorenko, E., Hsieh, P.-J., Nieto-Castañón, A., Whitfield-Gabrieli, S. & Kanwisher, N.  
416 New method for fMRI investigations of language: defining ROIs functionally in individual  
417 subjects. *J. Neurophysiol.* **104**, 1177-1194 (2010).
- 418 44. Desikan, R.S., *et al.* An automated labeling system for subdividing the human cerebral  
419 cortex on MRI scans into gyral based regions of interest. **31**, 968-980 (2006).
- 420 45. Fedorenko, E., Duncan, J. & Kanwisher, N. Broad domain generality in focal regions of  
421 frontal and parietal cortex. *Proc Natl Acad Sci USA.* **110**, 16616-16621 (2013).

- 422 46. Julian, J.B., Fedorenko, E., Webster, J. & Kanwisher, N. An algorithmic method for  
423 functionally defining regions of interest in the ventral visual pathway. *Neuroimage*. **60**, 2357-  
424 2364 (2012).
- 425 47. Pitcher, D., Dilks, D.D., Saxe, R.R., Triantafyllou, C. & Kanwisher, N. Differential  
426 selectivity for dynamic versus static information in face-selective cortical regions. *Neuroimage*.  
427 **56**, 2356-2363 (2011).
- 428 48. McCarthy, G., Puce, A., Gore, J.C. & Allison, T. Face-specific processing in the human  
429 fusiform gyrus. *J Cogn Neurosci*. **9**, 605-610 (1997).
- 430 49. Kanwisher, N., McDermott, J. & Chun, M.M. The fusiform face area: a module in human  
431 extrastriate cortex specialized for face perception. *J Neurosci*. **17**, 4302-4311 (1997).
- 432 50. Gauthier, I., *et al.* The fusiform “face area” is part of a network that processes faces at the  
433 individual level. *J Cogn Neurosci*. **12**, 495-504 (2000).
- 434 51. Epstein, R. & Kanwisher, N. A cortical representation of the local visual environment.  
435 *Nature*. **392**, 598-601 (1998).
- 436 52. Grill-Spector, K., *et al.* Differential processing of objects under various viewing  
437 conditions in the human lateral occipital complex. *Neuron*. **24**, 187-203 (1999).
- 438 53. Frost, J.A., *et al.* Language processing is strongly left lateralized in both sexes: Evidence  
439 from functional MRI. *Brain*. **122**, 199-208 (1999).
- 440 54. Wang, H. & Yushkevich, P. Multi-atlas segmentation with joint label fusion and  
441 corrective learning—an open source implementation. *Front Neuroinform*. **7**, 27 (2013).
- 442 55. Menze, B.H., *et al.* The multimodal brain tumor image segmentation benchmark  
443 (BRATS). *IEEE Trans Med Imaging*. **34**, 1993-2024 (2014).

444 56. Avants, B.B., *et al.* The Insight ToolKit image registration framework. *Front*  
445 *Neuroinform.* **8**, 44 (2014).

446

## 447 **Online Methods**

### 448 **Participants.**

449 *Neonates.* We used the initial release of the Developing Human Connectome Project  
450 (dHCP) neonatal data (<http://www.developingconnectome.org>)<sup>33</sup>. Neonates were  
451 recruited and imaged at the Evelina Neonatal Imaging Centre, London. Informed  
452 parental consent was obtained for imaging and data release, and the study was  
453 approved by the UK Health Research Authority. 39 neonates were included in functional  
454 connectivity analysis and were born and imaged at term age (14 female, mean  
455 gestational age at birth = 39.03 weeks, gestational age range at scan = 37-44 weeks).

456 *Adults.* Adult data were obtained from the Human Connectome Project (HCP), WU-Minn  
457 HCP 1200 Subjects Data Release ([https://www.humanconnectome.org/study/hcp-](https://www.humanconnectome.org/study/hcp-young-adult)  
458 [young-adult](https://www.humanconnectome.org/study/hcp-young-adult))<sup>34</sup>. All participants were scanned at Washington University in St. Louis  
459 (WashU). 38 adults were included in functional connectivity analysis (19 female, age  
460 range = 22-36 years old).

461

### 462 **Data acquisition.**

463 *Neonates.*

464 Imaging was carried out on 3T Philips Achieva (running modified R3.2.2 software) using  
465 a dedicated neonatal imaging system which included a neonatal 32 channel phased  
466 array head coil<sup>35</sup>. All neonates were scanned in natural sleep.

467 **Resting-state fMRI.** High temporal resolution fMRI developed for neonates using  
468 multiband (MB) 9x accelerated echo-planar imaging was collected (TE/TR = 38/392ms,  
469 voxel size = 2.15 × 2.15 × 2.15mm<sup>3</sup>). The duration of resting-state fMRI scanning was  
470 approximately 15 minutes and consisted of 2300 volumes for each run. No in-plane  
471 acceleration or partial Fourier was used. Single-band reference scans were also  
472 acquired with bandwidth matched readout, along with additional spin-echo acquisitions  
473 with both AP/PA fold-over encoding directions.

474 **Anatomical MRI.** High-resolution T2-weighted and inversion recovery T1-weighted  
475 multi-slice fast spin-echo images were acquired with in-plane resolution 0.8 × 0.8mm<sup>2</sup>  
476 and 1.6mm slices overlapped by 0.8mm (T2-weighted: TE/TR = 156/12000ms; T1  
477 weighted: TE/TR/TI = 8.7/4795/1740ms).

478 *Adults.*

479 All the scans of WU-Minn HCP 1200 Subjects Data Release was carried out using a  
480 customized 3T Connectome Scanner adapted from a Siemens Skyra (Siemens AG,  
481 Erlanger, Germany) with 32-channel Siemens receive head coil and a “body”  
482 transmission coil designed by Siemens specifically for the smaller space available using  
483 the special gradients for the WU-Minn and MGH-UCLA Connectome scanners.

484 **Resting-state fMRI.** Participants were scanned using the Gradient-echo EPI sequence  
485 (TE/TR = 33.1/720ms, flip angle = 52°, number of slices = 72, voxel size = 2 × 2 × 2  
486 mm<sup>3</sup>). The duration of resting-state fMRI scanning was approximately 15 minutes and  
487 consisted of 1200 volumes for each run. All participants accomplished two resting-state  
488 fMRI sessions. Within each session, there were two phases encoding in a right-to-left  
489 (RL) direction in one run and phase encoding in a left-to-right (LR) direction in the other  
490 run. In current analysis, we used the LR phase encoding from the first session.

491 Participants were instructed to open their eyes with relaxed fixation on a projected bright  
492 cross-hair on a dark background.

493 **Anatomical MRI.** High-resolution T2-weighted and T1-weighted images were acquired  
494 with isotropic voxel resolution of 0.7mm<sup>3</sup> (T2-weighted 3D T2-SPACE scan: TE/TR =  
495 565/3200ms; T1-weighted 3D MPRAGE: TE/TR/TI = 2.14/2400/1000ms)

496

## 497 **Preprocessing.**

498 *Neonates.*

499 The dHCP data were preprocessed using the dHCP minimal processing pipelines. For  
500 anatomical MRI data segmentation, the minimal preprocessing<sup>33</sup> included bias  
501 correction, brain extraction using BET from FSL, and segmentation of the T2w volume  
502 using DRAW-EM algorithm<sup>36</sup>. In addition, a dedicated infant processing pipeline<sup>37, 38</sup> in  
503 FreeSurfer v.6.0.0 (<http://surfer.nmr.mgh.harvard.edu/fswiki/infantFS>) was implemented  
504 to get a gray/white matter mask.



505 For resting-state fMRI data, the minimal preprocessing included the following  
506 steps<sup>39</sup>: distortion-correction, motion correction, 2-stage registration of the MB-EPI  
507 functional image to T2 structural image and also generate combined transform from  
508 MB-EPI to 40-week T2 template, temporal high-pass filter (150s high-pass cutoff), and  
509 ICA denoising using FSL FIX<sup>40</sup>. With the minimally preprocessed data, we additionally  
510 applied smoothing (Gaussian filter with the FWHM = 3 mm) within the all gray matter,  
511 and band-pass filter at 0.009-0.08 Hz. As a further denoising step, we used  
512 aCompCor<sup>41</sup> to regress out signals from white matter and cerebrospinal fluid (CSF) to  
513 control the physiological noise like respiration and heartbeat as well as non-neuronal  
514 contributions to the resting state signal. All the FC analyses for the neonatal group were  
515 performed in native functional space.

#### 516 *Adults.*

517 The HCP data were preprocessed using the HCP minimal preprocessing pipelines<sup>42</sup>.  
518 For anatomical data, a PreFreeSurfer pipeline was applied to correct gradient distortion,  
519 produce an undistorted “native” structural volume space for each participant by ACPC  
520 registration, extract the brain, perform a bias field correction, and register the T2-  
521 weighted scan to the T1-weighted scan. Each individual brain was also aligned to  
522 common MNI152 template (with 0.7mm isotropic resolution). Then, the FreeSurfer  
523 pipeline (based on FreeSurfer 5.3.0-HCP) was performed with a number of  
524 enhancements specifically designed to capitalize on HCP data<sup>42</sup>. The main goals of this  
525 pipeline are to segment the volume into predefined structures, reconstruct white and

526 pial cortical surfaces, and perform FreeSurfer's standard folding-based surface  
527 registration to their surface atlas (fsaverage).

528 For resting-state fMRI data, the minimal functional analysis pipelines included the  
529 following steps: removed spatial distortions, corrected for motion, registered the fMRI  
530 data to both structural and MNI152 template, reduced the bias field, normalized the 4D  
531 image to a global mean, and masked the data with the final brain mask. After, the data  
532 were further denoised using the novel ICA-FIX method<sup>40</sup>. In order to preprocess these  
533 data in a pipeline that mirrored the neonatal group, we unwarped the data from MNI152  
534 to native space, as the dHCP preprocessing pipeline did not perform this  
535 transformation. Just as the neonatal group, we then applied spatial smoothing  
536 (Gaussian filter with the FWHM = 3 mm) within all gray matter, band-pass filtered at  
537 0.009-0.08 Hz, and implemented aCompCor.

538

### 539 **Defining the functional parcels.**

540 The VWFA parcel, located in left occipitotemporal cortex, was created from 20 adults  
541 (10 female, mean age = 24.6 years) by combining the 10% most responsive voxels in  
542 each adult that showed higher activation to words than line drawing objects<sup>22</sup>. The  
543 language parcels were released by Fedorenko et al. using a sentences vs. non-words  
544 contrast and created based on a probabilistic overlap map from 25 participants<sup>43</sup>. We  
545 used seven key language parcels in left inferior frontal and left temporal cortex in the  
546 present study. We defined a speech parcel in superior temporal sulcus by overlapping

547 13 adults' speech ROIs (auditorily-presented English sentences vs. scrambled  
548 sentences contrast), and keeping the voxels where at least 6 of the 13 adults  
549 overlapped. We defined A1 using superior and transverse temporal cortex from the  
550 FreeSurfer Desikan-Killiany parcellation<sup>44</sup> in CVS average-35 MNI152 space. A set of  
551 multiple-demand (MD) parcels located in left frontal cortex were defined by higher  
552 response to a hard condition compared to an easy condition in a variety of cognitive  
553 tasks<sup>45</sup>. High-level visual parcels used in the present study were derived from Julian et  
554 al.<sup>46</sup>, which were identified based on a group of adults (n = 40) with a dynamic movie  
555 clips localizer<sup>47</sup>. For the face selective parcels, FFA and OFA were identified with  
556 faces > objects contrasts<sup>48-50</sup>; for the scene selective parcel, PPA was identified with  
557 scenes > objects contrasts<sup>51</sup>; for the object selective parcels, LO and PFS were defined  
558 with objects > scrambled objects contrasts<sup>52</sup>. Because both VWFA and language are  
559 largely left lateralized<sup>30, 53</sup>, our study includes left hemisphere seeds and targets only.

560 All functional parcels were originally in CVS average-35 MNI152 space, and were  
561 overlaid onto each individual's native anatomical brain using Advanced Normalization  
562 Tools (ANTs version 2.1.0; <http://stnava.github.io/ANTs>)<sup>54-56</sup> for both adults and  
563 neonates. We further converted the parcels to native functional space using nearest  
564 neighbor interpolation with Freesurfer's `mri_vol2vol` function  
565 ([https://surfer.nmr.mgh.harvard.edu/fswiki/mri\\_vol2vol](https://surfer.nmr.mgh.harvard.edu/fswiki/mri_vol2vol)).

566 To ensure no voxel belonged to more than one functional parcel, we assigned any  
567 intersecting voxels of two functional parcels to the one with smaller size. Additionally,

568 voxels within white matter and cerebellum were also removed. In total, we used 17 non-  
569 overlapping functional parcels from eight categories in the present study.

570

### 571 **Calculating functional connectivity.**

572 The mean timecourse of each functional parcel was computed from the preprocessed  
573 resting state images, and FC was calculated with Pearson's correlation between the  
574 mean timecourse of each seed parcel and each target parcel. To generate normally  
575 distributed values, each FC value was Fisher z-transformed.

576

### 577 **FC fingerprint plots**

578 First, we calculated the averaged FC from seed to each of the target category. Then we  
579 subtracted the mean FC across all categories from each of the averaged FC. Thus, the  
580 value in the fingerprint plots indicate how the seed connect to the target compared to  
581 the mean connections of seed to all categories.

582

### 583 **Voxel-wise FC analysis in the ventral temporal cortex (VTC).**

584 We performed a voxel-wise analysis across VTC to get a finer characterization of the  
585 connectivity pattern with language regions. We defined the VTC from the Desikan-  
586 Killiany parcellation<sup>44</sup>, including the fusiform and inferior temporal labels, in FreeSurfer

587 CVS average-35 MNI152 space, which were registered to each individual's anatomy.  
588 FC was computed between the mean timecourse of the language regions and the  
589 timecourse of each VTC voxel. Without predefining any functional parcels within the  
590 VTC, this analysis allowed us to characterize where the voxels with highest connectivity  
591 were located within the VTC.

## 592 **Statistics.**

593 Within-subject design (i.e., repeated-measures) was used, in which case no  
594 experimental group randomization or blinding in the present study. All *t* tests are paired  
595 and two-tailed. The 95% confidence interval of the mean FC true population was also  
596 reported for each *post hoc* paired *t* test. Data distribution was assumed to be normal,  
597 but this was not formally tested.

598 **Data availability.** The data and codes that support the findings of this study are  
599 available from the corresponding author upon request.